

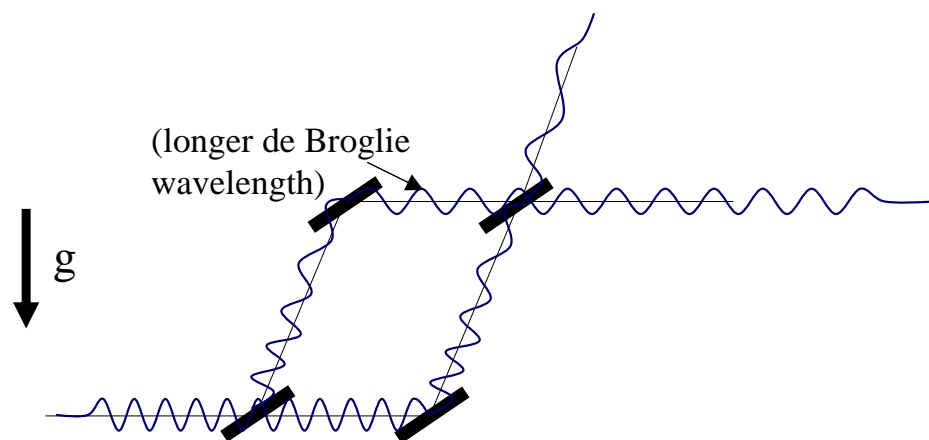
Navigation, Gravitation and Cosmology with Cold Atom Sensors

Atom Interferometry Group
Stanford Center for Position, Navigation and Time
Mark Kasevich

de Broglie wave sensors

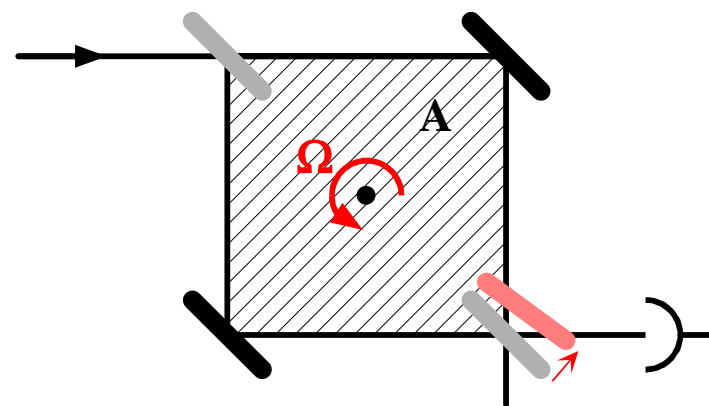
Gravity/Accelerations

As atom climbs gravitational potential, velocity decreases and wavelength increases



Rotations

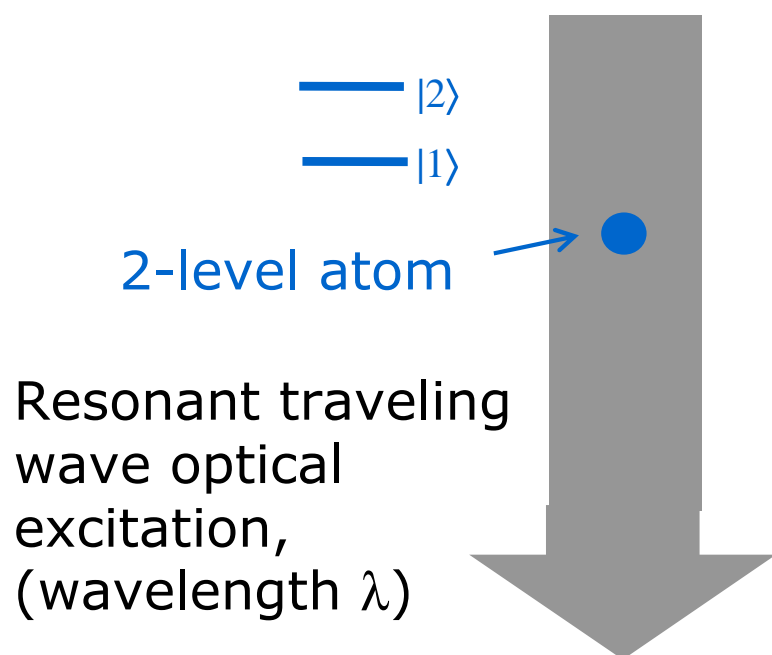
Sagnac effect for de Broglie waves



Current ground based experiments with atomic Cs:
wavepacket spatial separation ~ 1 cm, phase shift resolution $\sim 10^{-5}$ rad

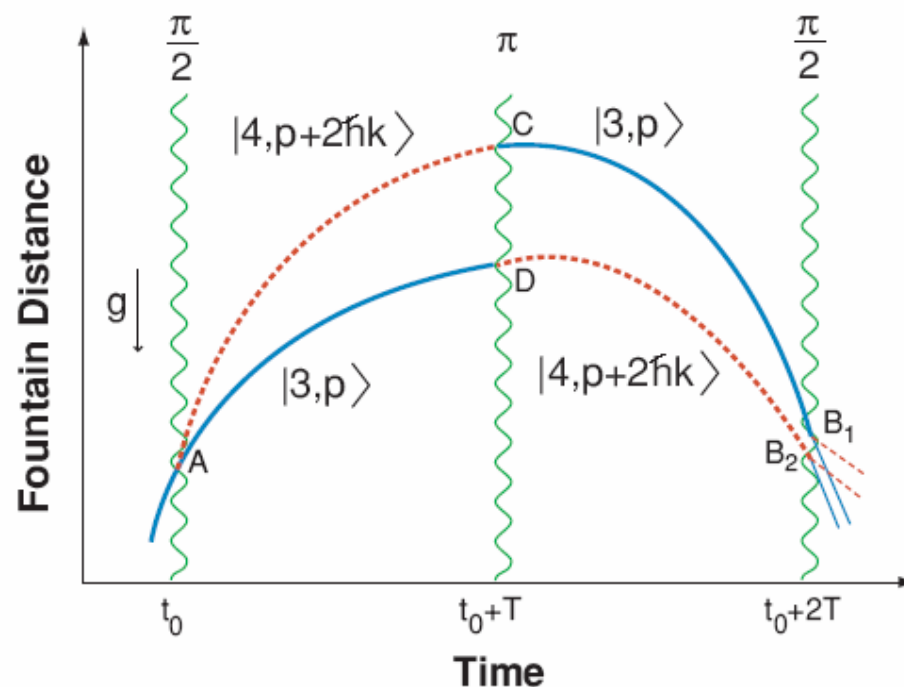
(Light-pulse) atom interferometry

Resonant optical interaction



Recoil diagram

Momentum conservation between atom and laser light field (recoil effects) leads to spatial separation of atomic wavepackets.



Enabling Science: Laser Cooling

Laser cooling techniques are used to achieve the required velocity (wavelength) control for the atom source.

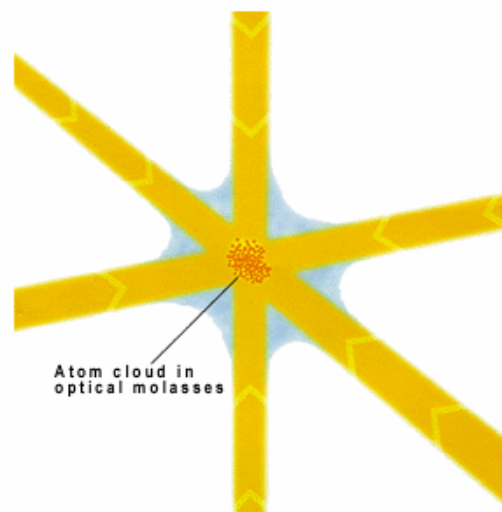


Image source: www.nobel.se/physics

Laser cooling:
Laser light is used to cool atomic vapors to temperatures of $\sim 10^{-6}$ deg K.



The Nobel Prize in Physics 1997

"for development of methods to cool and trap atoms with laser light"



Steven Chu



USA

Stanford University
Stanford, CA, USA

1948 -



Claude Cohen-Tannoudji



France

Collège de France
Paris, France
and École Normale Supérieure
Paris, France

1933 -



William D. Phillips

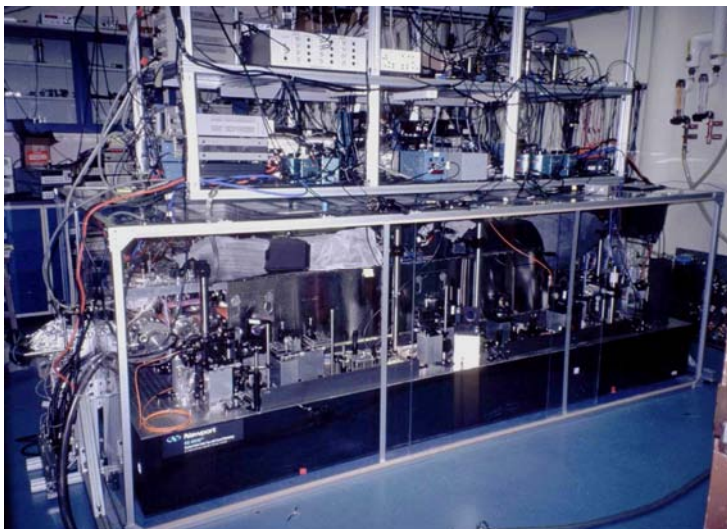


USA

National Institute of Standards and Technology
Gaithersburg, Maryland, USA

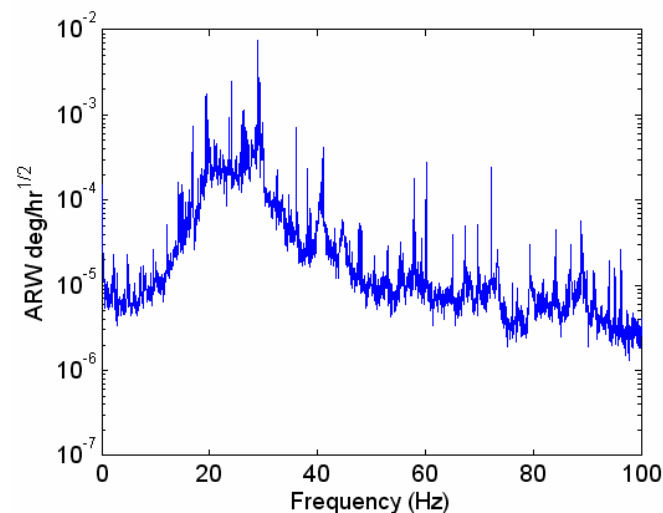
1948 -

Laboratory gyroscope

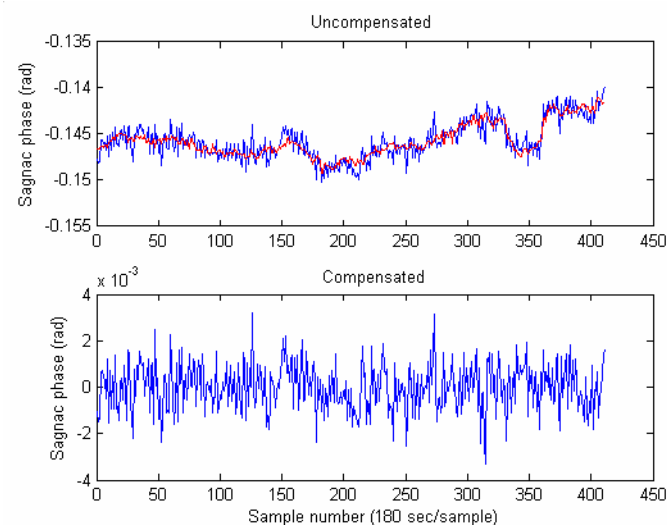


AI gyroscope

ARW **3 $\mu\text{deg/hr}^{1/2}$**
Bias stability: **< 60 $\mu\text{deg/hr}$**
Scale factor: **< 5 ppm**
(submitted for publication)

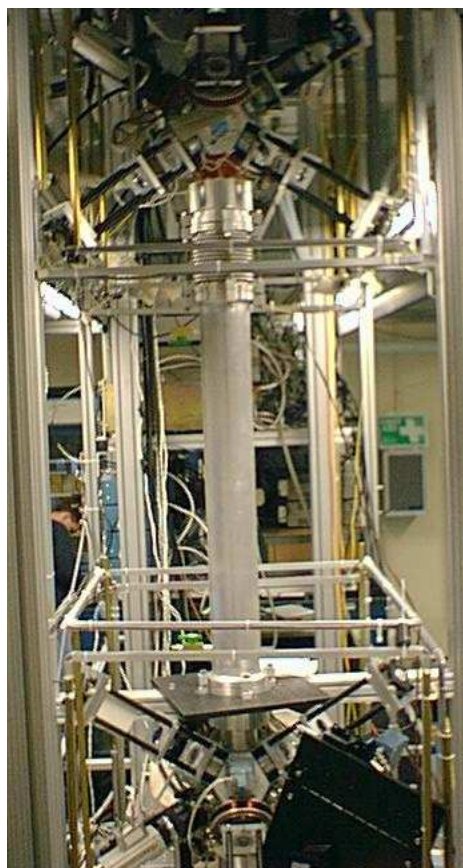
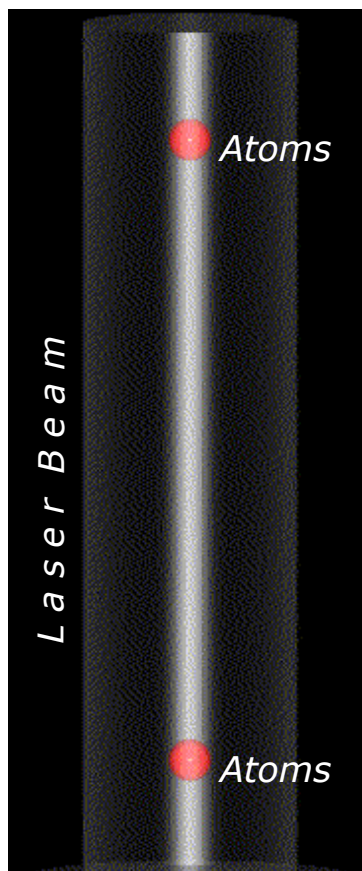


ARW

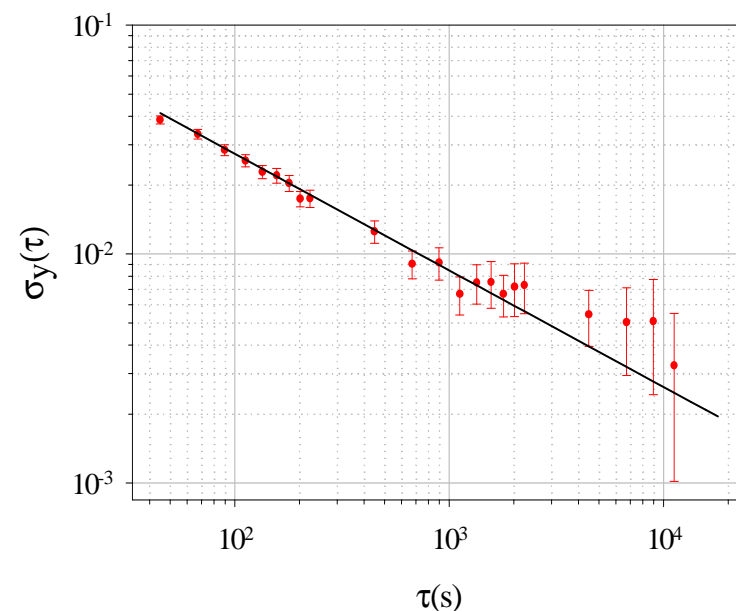


*Bias and
scale
factor
stability*

Laboratory gravity gradiometer



1.4 m



Demonstrated differential acceleration sensitivity:

$$4 \times 10^{-9} \text{ g/Hz}^{1/2}$$

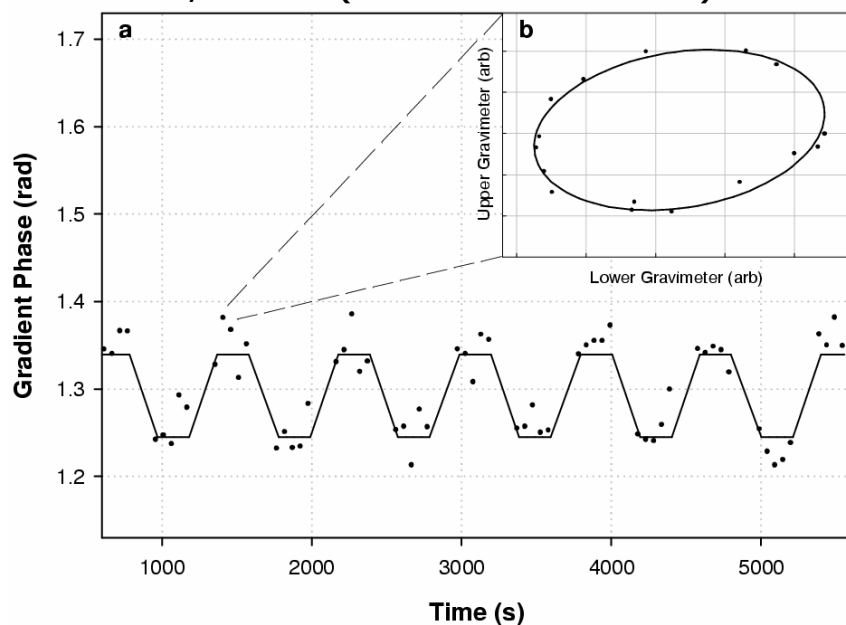
($2.8 \times 10^{-9} \text{ g/Hz}^{1/2}$ per accelerometer)

Distinguish gravity induced accelerations from those due to platform motion with differential acceleration measurements.

Gravity Gradiometer: Measurement of G



Yale, 2002 (Fixler PhD thesis)



Pb mass translated vertically along gradient measurement axis.

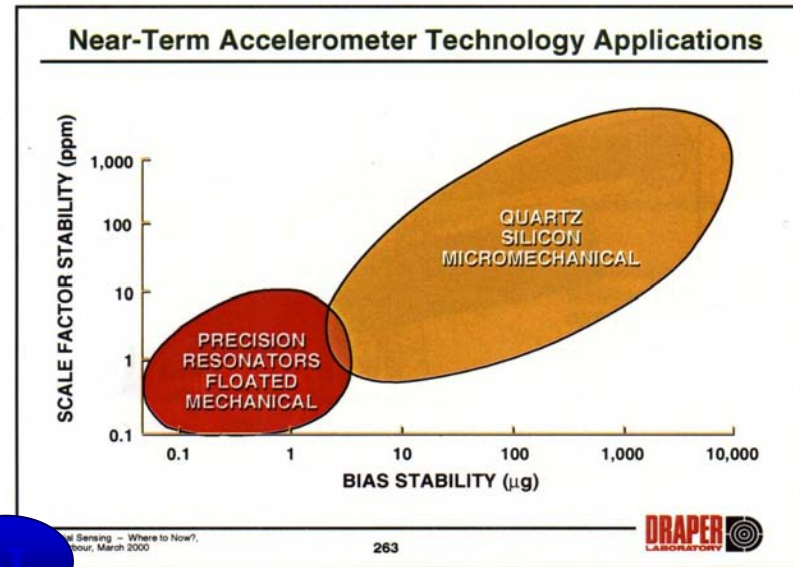
Systematic	$\frac{\delta G}{G}$
Initial Atom Velocity	1.88×10^{-3}
Initial Atom Position	1.85×10^{-3}
Pb Magnetic Field Gradients	1.00×10^{-3}
Rotations	0.98×10^{-3}
Source Positioning	0.82×10^{-3}
Source Mass Density	0.36×10^{-3}
Source Mass Dimensions	0.34×10^{-3}
Gravimeter Separation	0.19×10^{-3}
Source Mass Density inhomogeneity	0.16×10^{-3}
TOTAL	3.15×10^{-3}

Status: $\delta G/G \sim 3$ ppt (submitted for publication). See also Tino, MAGIA

Sensor characteristics

Light-pulse AI accelerometer characteristics

- Bias stability: $<10^{-10}$ g
- Noise: 4×10^{-9} g/Hz^{1/2}
- Scale Factor: 10^{-12}



Light-pulse AI gyroscope characteristics

- Bias stability: <60 μdeg/hr
- Noise (ARW): 4 μdeg/hr^{1/2}
- Scale Factor: <5 ppm

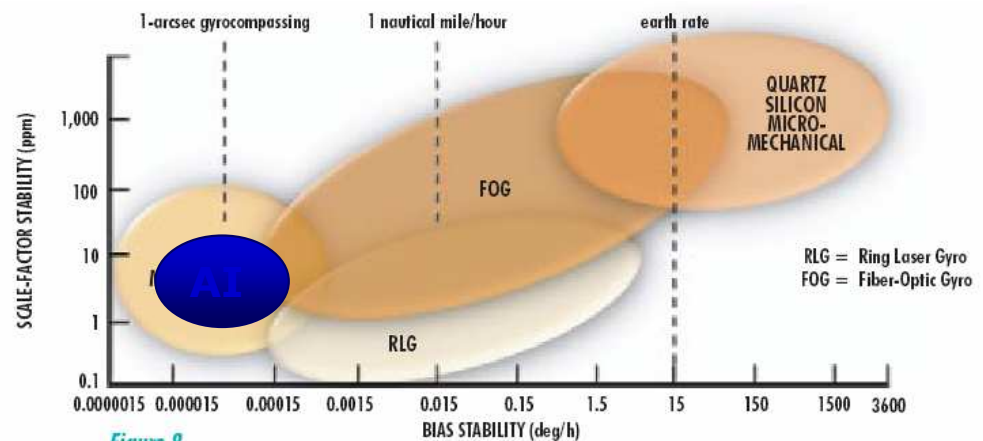


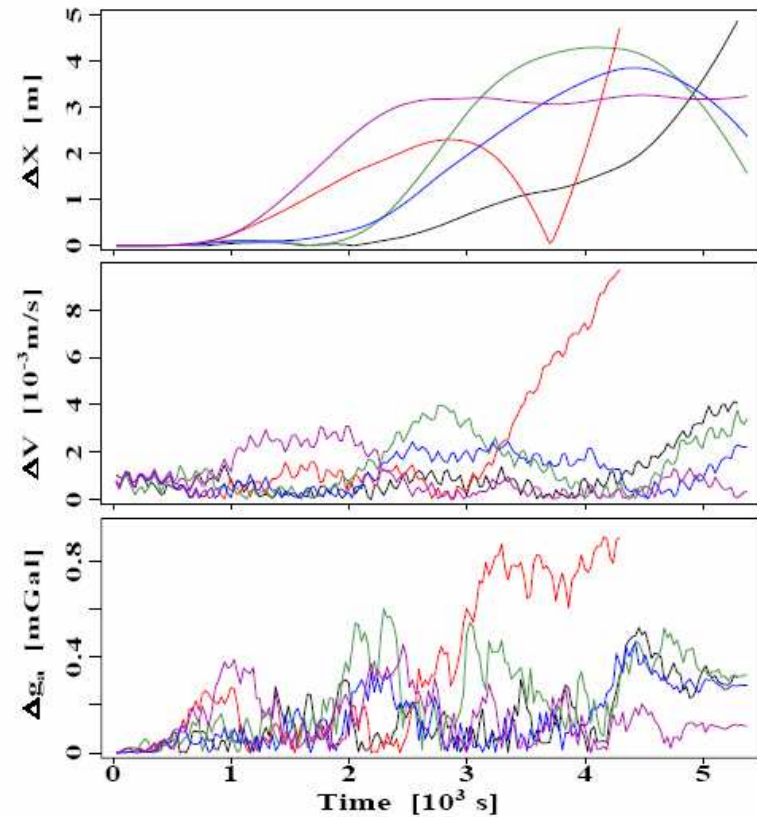
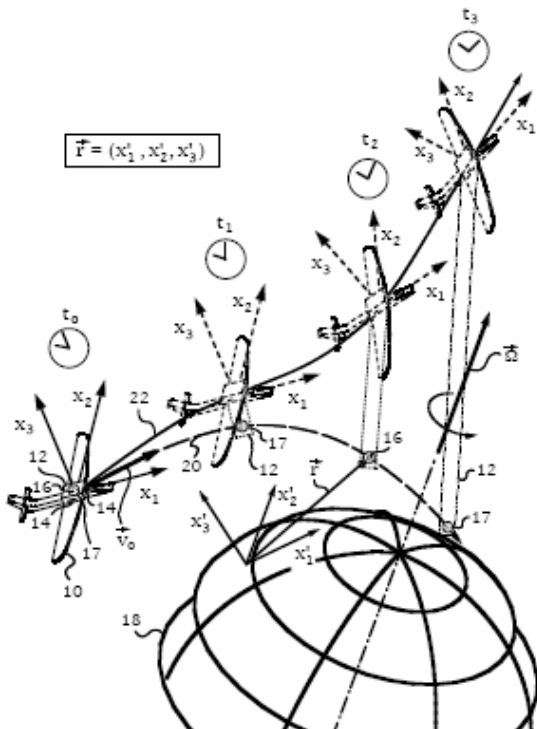
Figure 8

Source: Proc. IEEE/Workshop on Autonomous Underwater Vehicles

Navigation performance

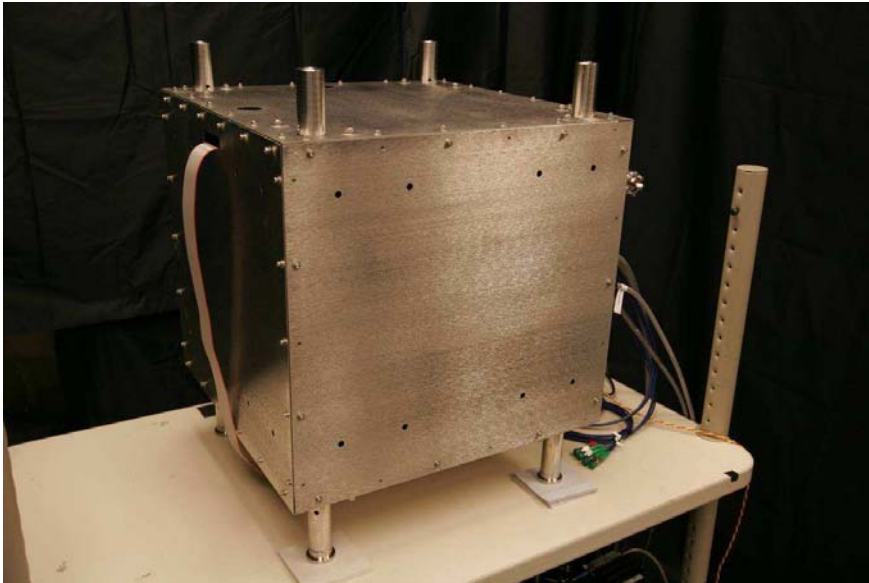
Determine geo-located platform path.

Necessarily involves geodetic inputs

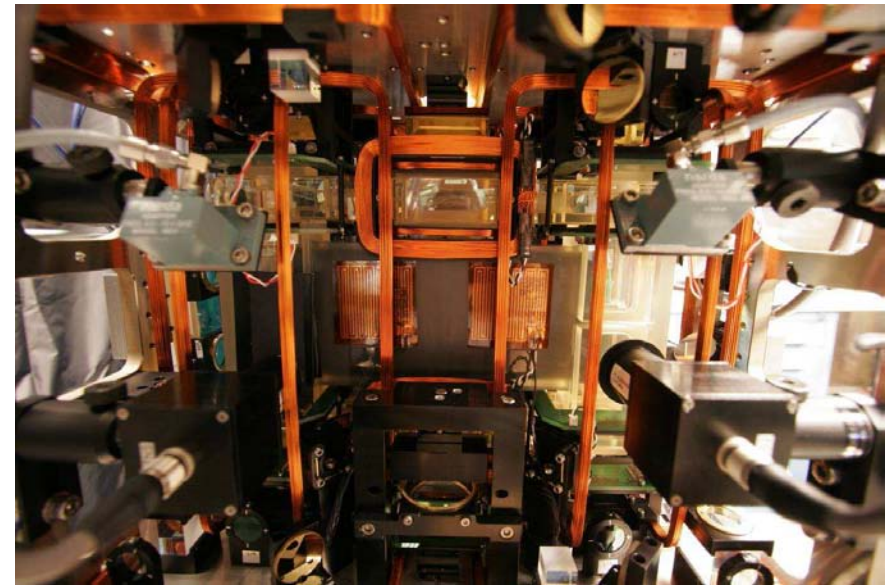


Simulated navigation solutions.
5 m/hr system drift demonstrated.

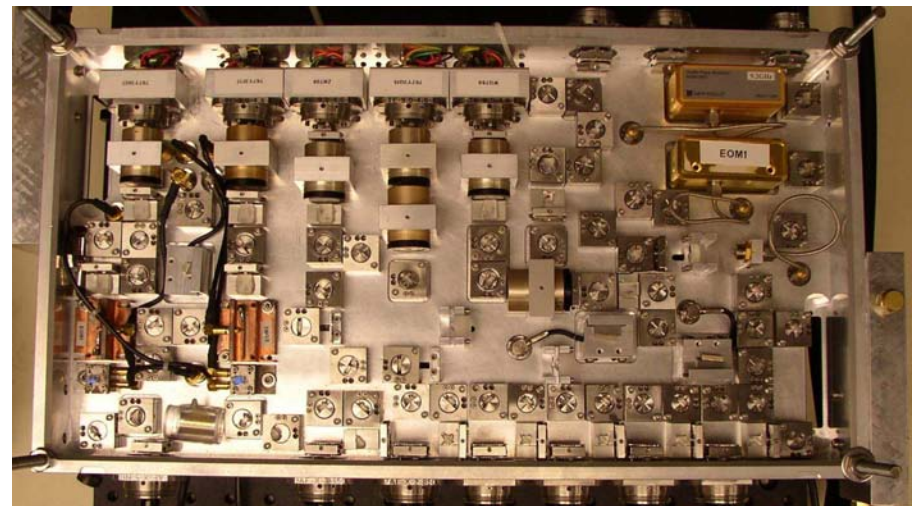
Compact gravity gradiometer/gyroscope/accelerometer



Multi-function sensor measures gravity gradient, rotation and linear acceleration along a single input axis.



Interior view

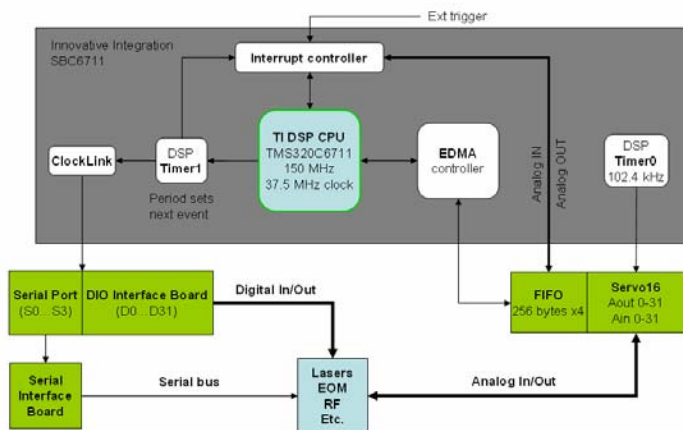


Laser system

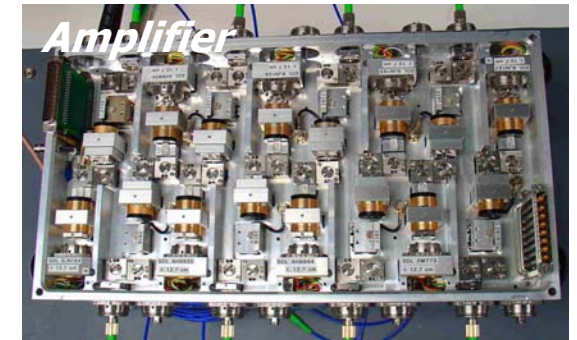
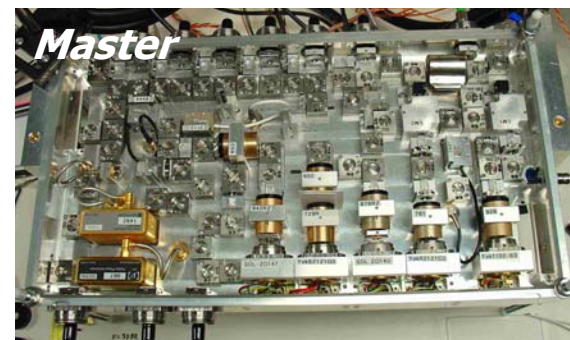
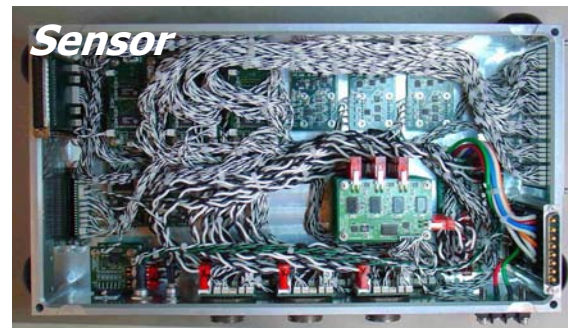
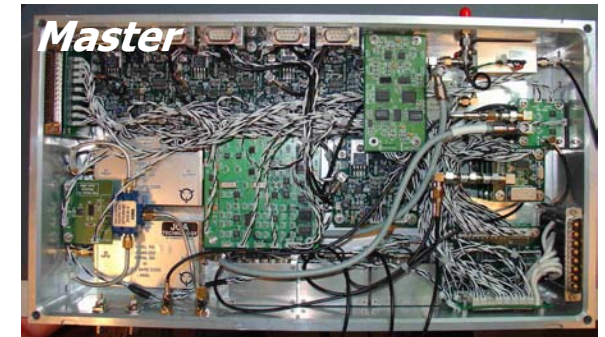
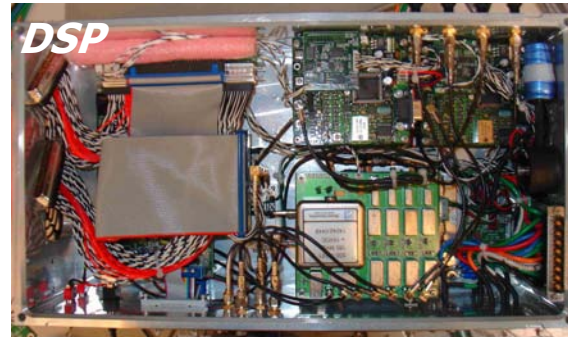


Sensor electronic/laser subsystems

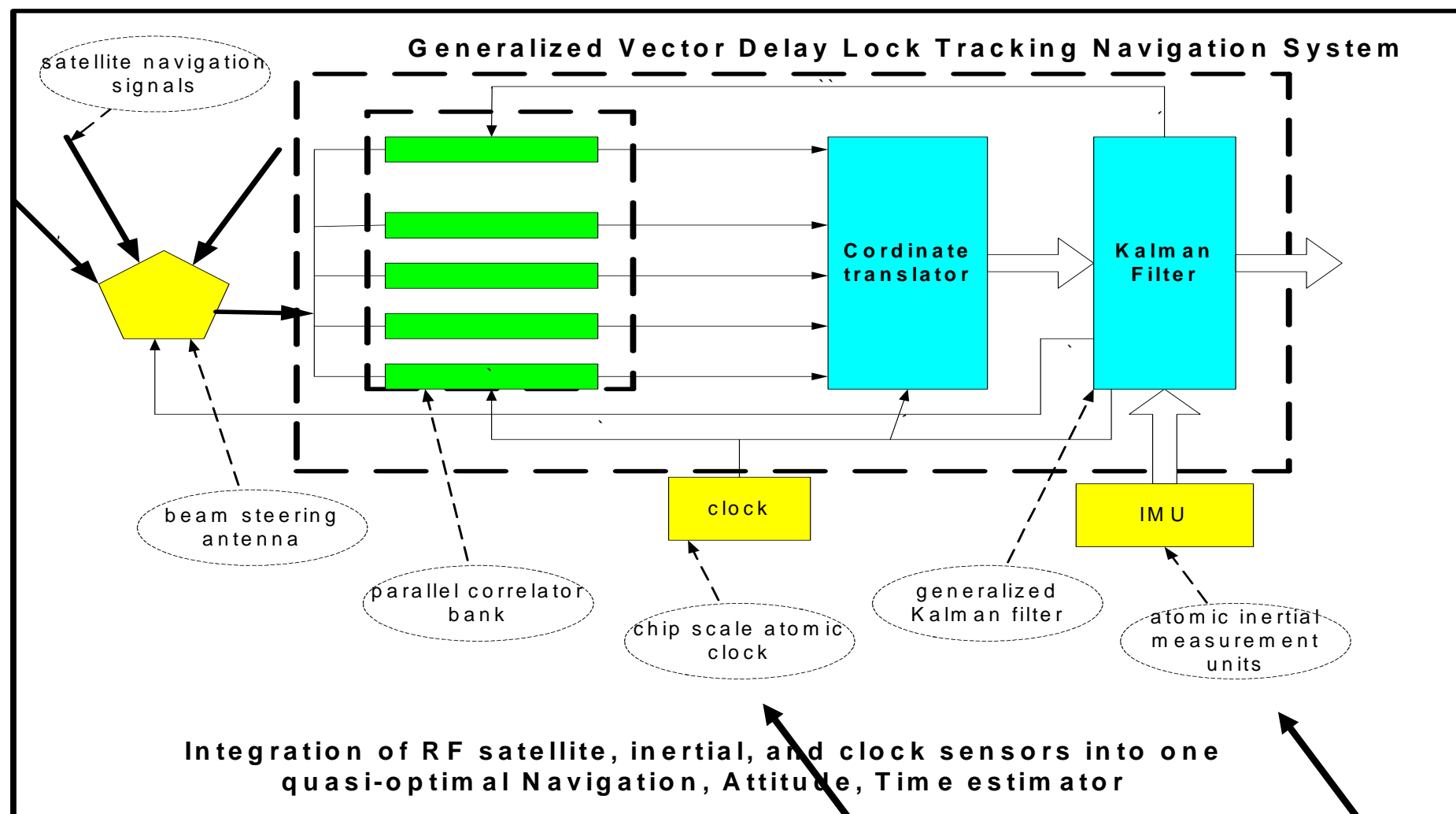
Control electronics frames
(controls 6 sensor heads)



Laser frames
(scalable architecture
provides light for 2-6
sensor heads)



Next generation integrated INS/GPS



*Stanford Center for Position, Navigation and Time.
In collaboration with Per Enge, Jim Spilker*

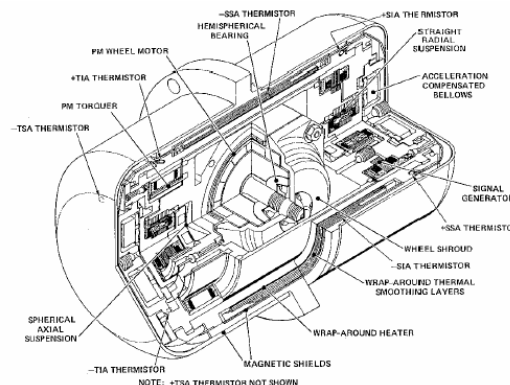
Atomic physics contributions

Space-based applications

- Platform jitter suppression
 - High resolution line-of-sight imaging from space
 - Inertial stabilization for next-generation telescopes
- Satellite drag force compensation at the 10^{-10} g accuracy level
 - GPS satellite drag compensation
 - Pioneer-type experiment
- Autonomous vehicle navigation, formation flying

Existing technology:

- *ESGN (submarine navigation)*
- *Draper LN-TGG gyro*
- *Litton/Northrop HRG (Hemispherical Resonator)*

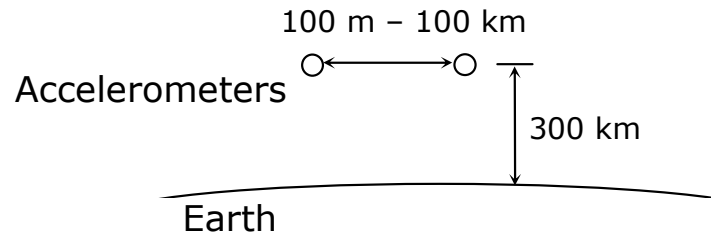


LN-TGG; 1 nrad 0.1-100 Hz
source: SPIE 4632-15



Fibersense/NG
IFOG

Space-based geodesy (also lunar geodesy)



Accelerometer sensitivity: 10^{-13} g/Hz^{1/2}
– Long free-fall times in orbit

Measurement baseline

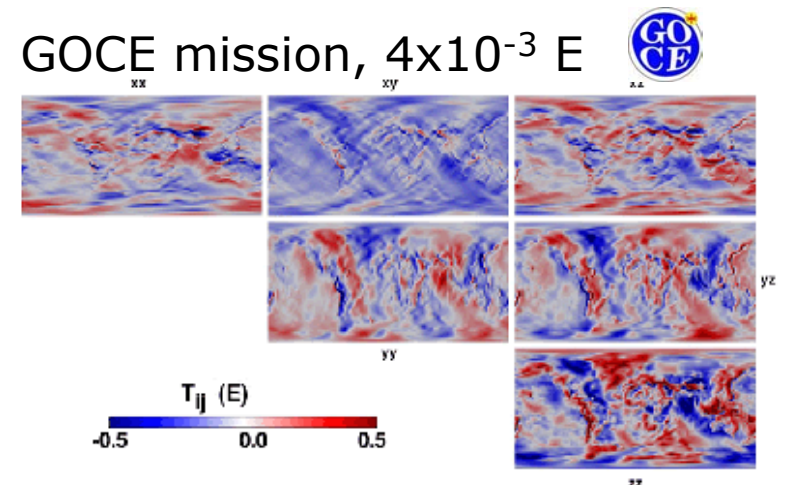
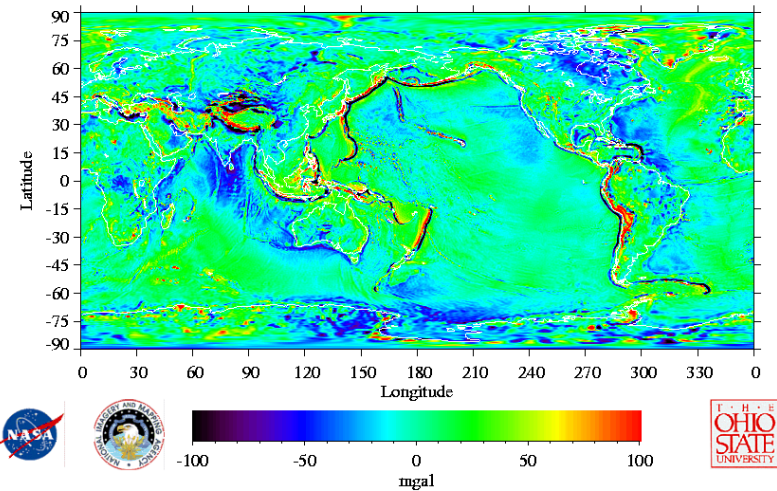
- 100 m (Space station)
- 100 km (Satellite constellation)

Sensitivity:

- 10^{-4} E/Hz^{1/2} (Space Station)
- 10^{-7} E/Hz^{1/2} (Satellite constellation)

Earthquake prediction; Water table monitoring

30' Mean Gravity Anomalies: EGM96 (Nmax=360)



<http://www.esa.int/export/esaLP/goce.html>

Equivalence Principle

Co-falling ^{85}Rb and ^{87}Rb ensembles

Evaporatively cool to $< 1 \mu\text{K}$ to enforce tight control over kinematic degrees of freedom

Statistical sensitivity

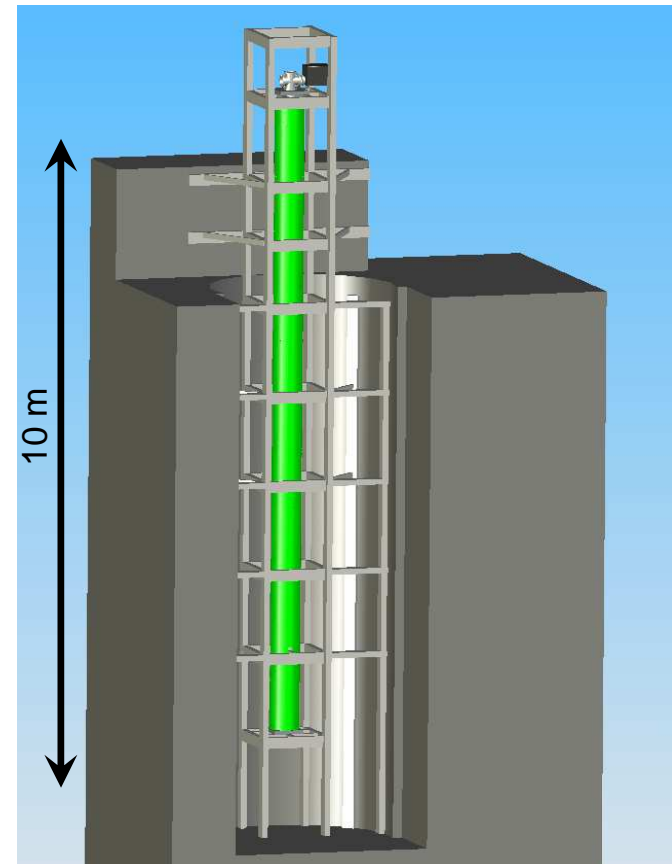
$\delta g \sim 10^{-15}$ with 1 month data collection

Systematic uncertainty

$\delta g \sim 10^{-16}$ limited by magnetic field inhomogeneities and gravity anomalies.

Also, new tests of General Relativity

Precursor to possible space-based system.



10 m atom drop tower.

~ 10 cm wavepacket separation (!)

Error Model

Use standard methods to analyze spurious phase shifts from uncontrolled:

- Rotations
- Gravity anomalies/gradients
- Magnetic fields
- Proof-mass overlap
- Misalignments
- Finite pulse effects

Known systematic effects appear controllable at the $\delta g \sim 10^{-16}$ level.

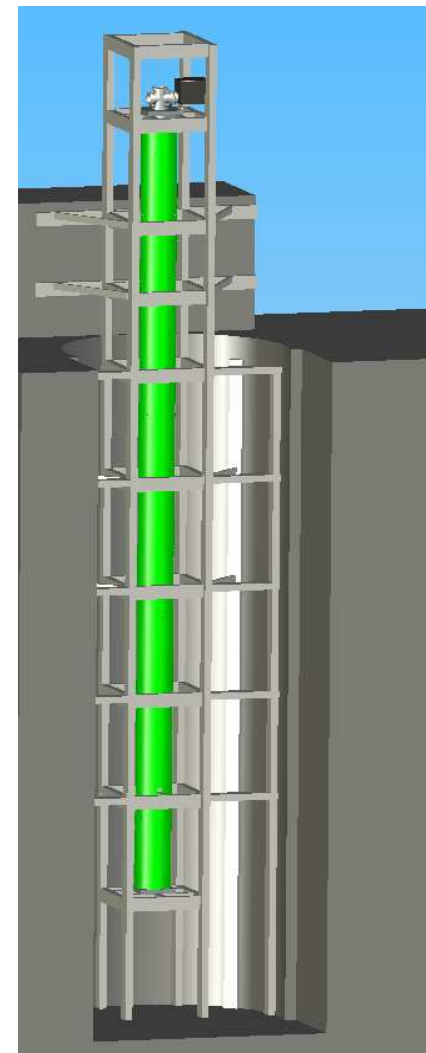
[$\delta G/G \sim 10^{-5}$ is feasible (limited by test mass)]

$-k_{\text{eff}} g T^2$	-2.84724×10^8	1.
$k_{\text{eff}} R_E \Omega_Y^2 T^2$	6.21045×10^5	2.18122×10^{-3}
$k_{\text{eff}} T_{zz} V_L T^3$	1.57836×10^3	5.54347×10^{-6}
$-\frac{7}{12} k_{\text{eff}} T_{zz} g T^4$	-9.20709×10^2	3.23369×10^{-6}
$2 k_{\text{eff}} v_{x0} \Omega_Y T^2$	1.97884×10^1	6.95002×10^{-6}
$-3 k_{\text{eff}} V_L \Omega_Y^2 T^3$	-5.16411	1.81373×10^{-6}
$\frac{7}{4} k_{\text{eff}} \Omega_Y^2 g T^4$	3.0124	1.05801×10^{-6}
$\frac{7}{12} k_{\text{eff}} R_E T_{zz} \Omega_Y^2 T^4$	2.00827	7.05338×10^{-9}
$\frac{k_{\text{eff}}^2 T_{zz} h T^3}{2m}$	7.05401×10^{-1}	2.47749×10^{-9}
$k_{\text{eff}} T_{zz} v_{z0} T^3$	7.05401×10^{-1}	2.47749×10^{-9}
$k_{\text{eff}} T_{zz} T^2 z_0$	8.92817×10^{-2}	3.13573×10^{-10}
$-\frac{7}{4} k_{\text{eff}} R_E \Omega_Y^4 T^4$	-6.57069×10^{-3}	2.30774×10^{-11}
$-\frac{7}{4} k_{\text{eff}} R_E \Omega_Y^2 \Omega_z^2 T^4$	-3.84744×10^{-3}	1.35129×10^{-11}
$-\frac{3 k_{\text{eff}}^2 \Omega_Y^2 h T^3}{2m}$	-2.30795×10^{-3}	8.10592×10^{-12}
$-3 k_{\text{eff}} v_{z0} \Omega_Y^2 T^3$	-2.30795×10^{-3}	8.10592×10^{-12}
$\frac{1}{4} k_{\text{eff}} T_{zz}^2 V_L T^5$	2.18739×10^{-3}	7.68251×10^{-12}
$3 k_{\text{eff}} v_{y0} \Omega_Y \Omega_z T^3$	1.76607×10^{-3}	6.20273×10^{-12}
$-\frac{31}{360} k_{\text{eff}} T_{zz}^2 g T^6$	-7.53436×10^{-4}	2.6462×10^{-12}
$4 B_0 V_L T^2 \alpha b_{z1}$	5.14655×10^{-4}	1.80756×10^{-12}
$-4 B_0 g T^3 \alpha b_{z1}$	-5.14655×10^{-4}	1.80756×10^{-12}
$k_{\text{eff}} \Omega_Y^2 T^2 z_0$	9.73714×10^{-5}	3.41985×10^{-13}
$-k_{\text{eff}} \Omega_Y \Omega_z T^2 y_0$	-7.45096×10^{-5}	2.61691×10^{-13}
$\frac{7}{6} k_{\text{eff}} T_{zz} v_{x0} \Omega_Y T^4$	6.39894×10^{-5}	2.24742×10^{-13}
$-7 V_L g T^4 \alpha b_{z1}^2$	-4.7766×10^{-5}	1.67762×10^{-13}
$\frac{7}{6} k_{\text{eff}} T_{zz} v_{x0} \Omega_Y T^4$	-3.19947×10^{-5}	1.12371×10^{-13}
$4 V_L^2 T^3 \alpha b_{z1}^2$	2.72948×10^{-5}	9.58642×10^{-14}
$3 g^2 T^5 \alpha b_{z1}^2$	2.04711×10^{-5}	7.18982×10^{-14}
...

Equivalence Principle Installation



Atomic source



10 m atom drop tower.

Gravitation

Light-pulse interferometer phase shifts for Schwarzschild metric:

- Geodesic propagation for atoms and light.
- Path integral formulation to obtain quantum phases.
- Atom-field interaction at intersection of laser and atom geodesics.

Objective:

Ground-based precision tests of post-Newtonian gravity.

Post-Newtonian trajectories for classical particle:

$$\frac{d\mathbf{v}}{dt} = -\nabla(\phi + 2\phi^2 + \psi) - \frac{\partial \zeta}{\partial t} + \mathbf{v} \times (\nabla \times \zeta) + 3\mathbf{v} \frac{\partial \phi}{\partial t} + 4\mathbf{v}(\mathbf{v} \cdot \nabla)\phi - v^2 \nabla \phi$$

From Weinberg, Eq. 9.2.1

Prior work, de Broglie interferometry: Post-Newtonian effects of gravity on quantum interferometry, Shigeru Wajima, Masumi Kasai, Toshifumi Futamase, Phys. Rev. D, 55, 1997; Bordé, et al.



Ground-based Post-Newtonian Interferometry

Calculated phase shifts for **ground based**, 10 m, apparatus.

- Analysis indicates that several post-Newtonian terms are comfortably within apparatus reach.
- In-line, accelerometer, configuration (milliarcsec link to external frame NOT req'd).
- New constraints of PPN parameters.
- Identification of most-promising space-based tests.

Collaborators: Savas Dimopoulos, Peter Graham, Jason Hogan.

$\frac{GM\text{keff}T^2}{r\text{laser}^2}$	$1. \times 10^8$
$-\frac{2GM\text{keff}T^3vLr}{r\text{laser}^3}$	-2000.
$-\frac{GMT^2\omega_{\text{eff}}}{r\text{laser}^2}$	-1000.
$\frac{GMT^2\omega A}{r\text{laser}^2}$	1000.
$\frac{7GM^2\text{keff}T^4}{6r\text{laser}^3}$	116.667
$\frac{3GM\text{keff}T^2vLr}{r\text{laser}^2}$	30.
$-\frac{3GM^2\text{keff}T^3}{r\text{laser}^4}$	-3.
$-\frac{GM\text{keff}^2T^3}{m r\text{laser}^3}$	-1.
$\frac{7GM\text{keff}T^4vLr^2}{2r\text{laser}^4}$	0.035
$\frac{2GMT^3vLr\omega_{\text{eff}}}{r\text{laser}^3}$	0.02
$-\frac{2GMT^3vLr\omega A}{r\text{laser}^3}$	-0.02
$\frac{3GM\text{keff}^2T^2}{2m r\text{laser}^4}$	0.015
$\frac{GM^2\text{keff}T^2}{r\text{laser}^3}$	0.01
$-\frac{11GM^2\text{keff}T^5vLr}{2r\text{laser}^6}$	-0.0055
$-\frac{7GM^2T^4\omega_{\text{eff}}}{6r\text{laser}^5}$	-0.00116667
$\frac{7GM^2T^4\omega A}{6r\text{laser}^5}$	0.00116667
$-\frac{8GM\text{keff}T^3vLr^2}{r\text{laser}^3}$	-0.0008
$-\frac{3GMT^2vLr\omega_{\text{eff}}}{r\text{laser}^2}$	-0.0003
$\frac{35GM^2\text{keff}T^4vLr}{2r\text{laser}^5}$	0.000175
$\frac{GMT^2vLr\omega A}{r\text{laser}^2}$	0.0001
$\frac{7GM\text{keff}^2T^4vLr}{2m r\text{laser}^4}$	0.000035



Cosmology

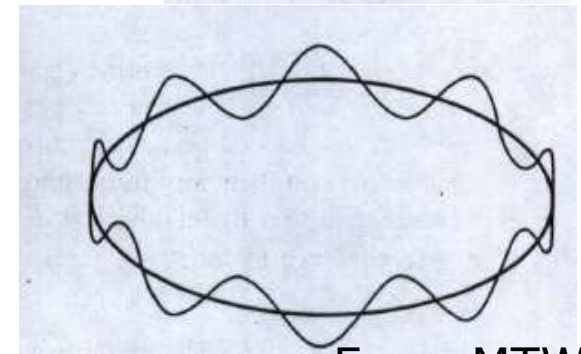
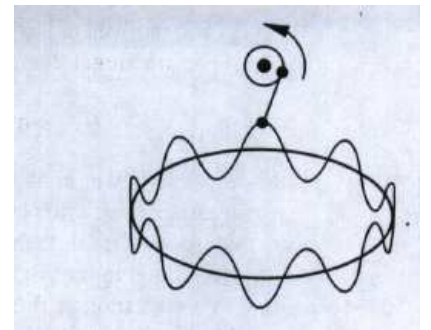
Are there (local) observable phase shifts of cosmological origin?

Analysis has been limited to simple metrics:

- FRW: $ds^2 = dt^2 - a(t)^2(dx^2 + dy^2 + dz^2)$
- McVittie: \sim Schwarzschild + FRW

$$g = \left(\frac{1 - m(t)/2r}{1 + m(t)/2r} \right)^2 dt^2 - \left(1 + \frac{m(t)}{2r} \right)^4 a^2(t) (dr^2 + r^2 d\Omega^2).$$

Giulini, gr-qc/0602098



From MTW

Work in progress ...

Future theory: Consider phenomenology of exotic/speculative theories (after validating methodology)

Collaborators: Savas Dimopoulos, Peter Graham, Jason Hogan.



Future technology: Quantum Metrology

Atom shot-noise limits sensor performance.

Recently evolving ideas in quantum information science have provided a road-map to exploit exotic quantum states to significantly enhance sensor performance.

- Sensor noise scales as $1/N$ where N is the number of particles
- “Heisenberg” limit
- Shot-noise $\sim 1/N^{1/2}$ limits existing sensors

Challenges:

- Demonstrate basic methods in laboratory
- Begin to address engineering tasks for realistic sensors

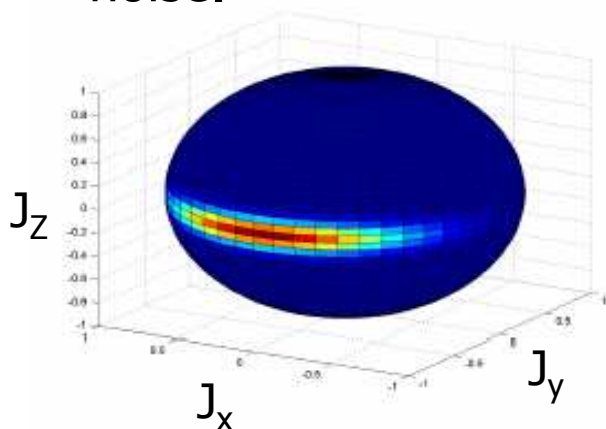
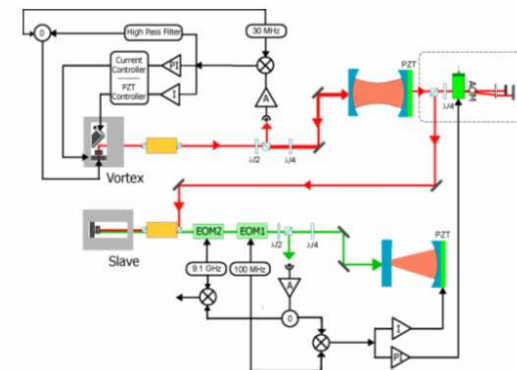
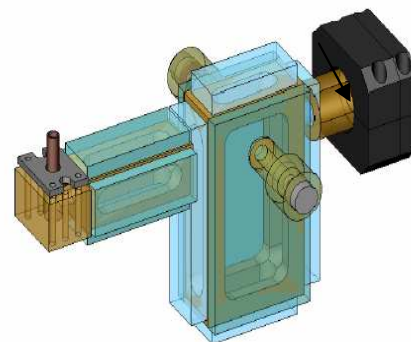
Impact of successful implementation for practical position/time sensors could be substantial.

Enables crucial trades for sensitivity, size and bandwidth.

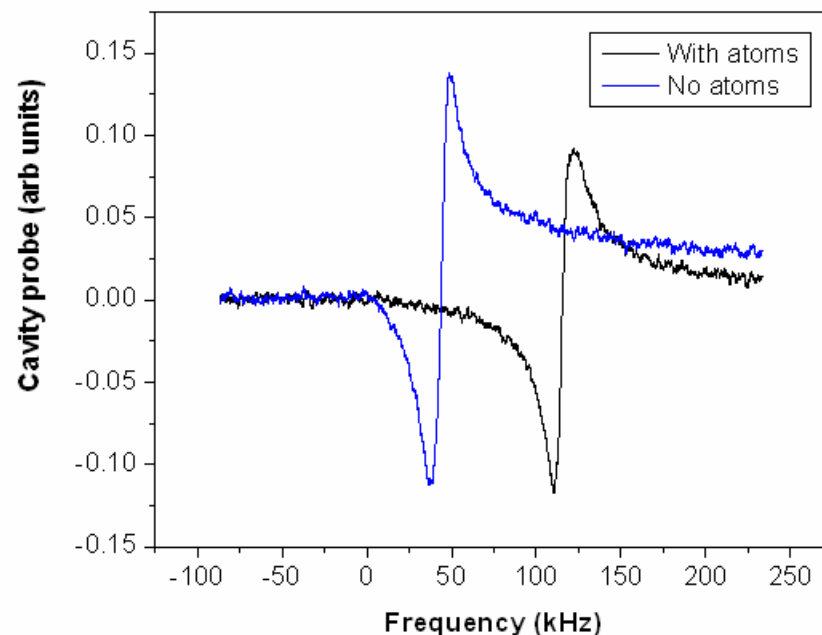


Quantum Metrology

- Exploit exotic quantum states to measure phase shifts at Heisenberg ($1/N$) limit
- CQED approach promising for precision sensors. Dispersive atom-cavity shifts enable requisite QND state preparation.
- Possible 10x to 100x improvement in sensor noise.



Spin squeezed state enables $1/N$ sensitivity



Possible QND detection of atom number (~ 5 atom resolution).



Summary

- Precision navigation
 - Pioneer
 - Equivalence Principle
 - Post-Newtonian gravity
 - Cosmology
-
- + quantum metrology in future sensor generations



Thanks

- Todd Gustavson, Research Scientist
- Boris Dubetsky, Research Scientist
- Todd Kawakami, Post-doctoral fellow
- Romain Long, Post-doctoral fellow
- Olaf Mandel, Post-doctoral fellow
- Peter Hommelhoff, Post-doctoral fellow
- Ari Tuchman, Research scientist
- Catherine Kealhofer, Graduate student, Physics
- Wei Li, Graduate student, Physics
- Hui-Chun Chen, Graduate student, Applied Physics
- Ruquan Wang, Graduate student, Physics
- Mingchang Liu, Graduate student, Physics
- Ken Takase, Graduate student, Physics
- Grant Biedermann, Graduate student, Physics
- Xinan Wu, Graduate student, Applied physics
- Jongmin Lee, Graduate student, Electrical engineering
- Chetan Mahadeswaraswamy, Graduate student, Mechanical engineering
- David Johnson, Graduate student, Aero/Astro engineering
- Geert Vrijzen, Graduate student, Applied physics
- Jason Hogan, Graduate student, Physics
- Nick Ciczek, Graduate student, Applied Physics
- Mike Minar, Graduate student, Applied Physics
- Sean Roy, Graduate student, Physics
- Larry Novak, Senior assembly technician
- Paul Bayer, Optomechanical engineer